

Preparation, characterization and statistical optimization of Nevirapine loaded chitosan nanoparticle for vaginal delivery

Sheikh Sofiur Rahman*, Abdul Baquee Ahmed

Department of Pharmaceutics, Girijananda Chowdhury Institute of Pharmaceutical Science, Hathkhowapara, Azara, Guwahati, Assam-781017.

Abstract

The purpose of the study was to develop a Nevirapine (NVP) loaded chitosan nanoparticles and optimize the formulation using 3^2 factorial designs for effective delivery of the drug for the treatment of HIV infection. Nevirapine loaded chitosan nanoparticles were prepared by salting out method and 3^2 randomized factorial designs were used to optimize the formulation. In this study, the concentration of chitosan (X1) and magnesium chloride (X2) were selected as independent variables and the particle size of the formulation (PS), % encapsulation efficiency (% EE), zeta potential and % drug release ($D_{Rel\ 8\ h}$) were selected as dependent variables. Drug-excipients compatibility studies were carried out by FR-IR and DSC. The result of FT-IR and DSC study confirmed the absence of incompatibility of NVP with excipients used in the formulations. Data obtained in these studies demonstrated that optimized formulation (MF6) showed particle size of 130 ± 3.15 nm with a low polydispersity index of 0.461 ± 0.002 , high EE of 83.02 ± 4.8 % and drug release of 94.55 ± 2.03 % at 8 hours. Zeta potential value of nanoparticles was found -17.12 mV and SEM images revealed the stability of nanoparticles. The rate of NVP permeation across porcine vaginal mucosa was found to be 168.05 ± 5.41 $\mu\text{m}/\text{cm}^2/\text{hr}$. In conclusion, stable nanoformulation was developed successfully with very good permeation of the drug across vaginal tissue that may increase the bioavailability in the target area thereby expected to increase the therapeutic effect NVP and will reduce the systemic toxicity.

Keywords: Nevirapine, chitosan nanoparticle, salting out, optimization, porcine vaginal mucosa.

1. INTRODUCTION

India has the third largest HIV epidemic in the world. In 2017, HIV prevalence among adults (aged 15-49) was an estimated 0.2%. This figure is small compared to most other middle-income countries but because of India's huge population (1.3 billion people), this equates to 2.1 million people living with HIV [1]. The prevalence of HIV, now a pandemic [2] is a big challenge to public health all over the world. Currently, it is accounted that 35 million people worldwide are HIV-positive, from which 19 million do not know that they have acquired the virus [3]. Although a significant decline in new HIV infections in the last decade was reported, the need for new innovative methodologies for HIV prevention is still a priority.

The HIV pandemic has motivated researchers to explore the development of new preventive technologies. A careful look at data collected from developing countries shows that the possibility that young women (up to 24 years old) are HIV-positive is 4 times higher compared to males in the same age group. In 2012, about 2 million new adult infections occurred, most of them in young people, especially young women in Africa. Such figures are common throughout developing countries and highlight the "vulnerability of women to HIV". The use of condoms (mainly men condoms) is currently the only method for HIV control in most countries, and this method is of course controlled by men (often women cannot insist for their use). Furthermore, condoms cannot be used by women who want to conceive. Intravaginally applied anti-HIV agents or nanoparticles (topical pre-exposure prophylaxis, PrEP), are the best alternatives to effective vaccines or oral PrEP, which provide women with an excellent opportunity to protect themselves. This is very important for women that due to cultural, social and/or economic reasons cannot use female condoms. Nanoparticles are topically applied drug

products which prevent HIV infection [3]. The word "nanoparticles" has the meaning of a substance which is administered vaginally (or in the rectum) in order to reduce the risk of sexually transmitted infection by HIV. Currently, no licensed nanoparticles are available, thereby the development of such type products prevail the unmet necessity for HIV prevention. Simple, low-cost and easy-to-use products could help women to control their own sexual/ reproductive health.

Nevirapine (NVP) is an excellent choice for the treatment of AIDS since it is a potent nonnucleoside reverse transcriptase inhibitor of human immunodeficiency virus type 1 (HIV-1), blocks polymerase activity after direct binding to the HIV-1 reverse transcriptase, resulting in the disruption of the enzyme's catalytic site. Moreover, it is the most important prescribed inhibitor of HIV-1 in the world and remains the most prescribed antiretroviral in countries with limited economic resources. However, NVP use has been associated with severe side effects that include hepatotoxicity, insomnia, confusion, memory loss, depression, rashes, nausea, dizziness, toxic epidermal necrolysis and hyperlipidemia. An alternative to enhance the clinical potential of NVP is the development of a drug delivery system that can lead to its sustained and target delivery [4].

In this work, we have attempted to develop chitosan nanoparticles loaded with NVP for vaginal application to increase the bioavailability of the drug in the targeted area to reduce systemic toxicity. 3^2 factorial design was used for statistical optimization of the delivery system and the prepared formulations were systematically characterized for various physicochemical parameters, *in-vitro* drug release and vaginal permeation of drug across porcine vaginal mucosa.

2. MATERIALS AND METHODS

2.1 Materials

NVP has obtained Astrix Laboratories Limited (Hyderabad, India) chitosan (CH), polyvinyl alcohol (PVA) and $MgCl_2$ were purchased from Sigma–Aldrich (St. Luis, USA). All chemicals and solvents used in this study were of analytical grade. HPLC-grade acetonitrile, methanol, potassium phthalate and ammonium acetate were purchased from Sigma–Aldrich (Steinheim, Germany). Glacial acetic acid (purity 99.8%) was obtained from Merck (Darmstadt, Germany). Phosphate buffer solution (pH 4.5) was prepared by mixing appropriate amounts of ammonium acetate and acetic acid.

3. METHODS

3.1 Experimental Design

A 3^2 randomized factorial design was used to optimize the NVP loaded Chitosan nanoparticles to achieve the desired particle size, high entrapment efficiency and controlled release of drug in vaginal fluid. In this study, the concentration of chitosan (X1) and magnesium chloride (X2) were selected as independent variables and the particle size of the formulation (PS), % encapsulation efficiency (% EE), zeta potential (ZP) and % drug release ($D_{Rel\ 8\ h}$) were selected as dependent variables. The high (+1), medium (0) and low (-1) levels for chitosan was used 40 mg, 30 mg and 20 mg; and that of salting agent ($MgCl_2$) the levels were 120 mg, 90 mg and 60 mg respectively. Table 1 summarized all the 9 experimental runs and Table 2 showed the actual composition of all the factorial batches formulation used for the study.

3.2 Preparation of drug-loaded nanoparticles

NVP loaded chitosan nanoparticles were prepared by salting out the method as per the composition is shown in Table 2. In brief, 200 mg of NVP and 20-40 mg of chitosan were dissolved in 30 ml of acetone at room temperature for 2 hours. The organic phase was then incorporated into a saturated aqueous solution of polyvinyl alcohol under magnetic stirring to form an o/w emulsion [5]. The resulting emulsion was stirred at 1000 rpm for 1 hr and subsequently homogenized at 24,000 rpm for 5 min using a high-speed homogenizer (IKA T25 digital Ultra Turrax, Germany). To this emulsion, water was added with constant stirring to facilitate diffusion and finally evaporate the organic solvent. This resulted in polymer precipitation and formation of nanoparticles. Free drug and surfactant were separated by centrifugation (REMI cooling centrifuge, Vasai) at $10,000\times g$ for 20 min.

3.3 Characterization of drug-loaded nanoparticles

3.3.1 Particle size and zeta potential

The particle size and the polydispersity index (PI) of the prepared nanoparticles were measured immediately by dynamic laser light scattering method at $25^\circ C$ at a scattering angle of 90° using Zetasizer Nano ZS 90 (Malvern Instruments Ltd. UK). The zeta potential of the preparations was also measured using the clear disposable Zeta cell for zeta potential analysis by electrophoretic

mobility method (Zetasizer ZS 90; Malvern Instruments Ltd. the UK) [6, 7].

3.3.2 Encapsulation efficiency

The freshly prepared chitosan nanoparticles were centrifuged at 20,000 rpm for 20 min at $5^\circ C$ temperature using cooling ultracentrifuge (REMI, cooling centrifuge, Vasai). The amount of unincorporated drug was measured by taking the absorbance of the appropriately diluted supernatant solution at 230 nm using UV spectrophotometer (Shimadzu UV-1800, Japan) against blank. Drug loading and encapsulation efficiency were calculated by using equation Eq. (1) and Eq. (2) respectively [8,9].

$$\% \text{ Drug Loading} = \frac{\text{Amount of drug in nanoparticle(mg)}}{\text{Amount of nanoparticle}} \quad \text{Eq..... (1)}$$

$$\% \text{ Encapsulation efficiency} = \frac{\text{Amount of drug in nanoparticle(mg)}}{\text{Initial amount of nanoparticle(mg)}} \quad \text{Eq.....(2)}$$

3.3.3 Drug-excipient compatibility study by FT-IR spectroscopy and Differential Scanning Calorimetry (DSC)

FT-IR spectra were recorded on a Bruker spectrophotometer (Model-220, Germany) in the range of $4000\text{--}400\text{ cm}^{-1}$. FT-IR analysis has been performed using a sample of NVP with various excipients at 1:1 mass/mass ratio used in the formulation [10,11].

A differential scanning calorimeter (Jade DSC, Perkin Elmer, USA) was used for thermal analysis of NVP and NVP-excipients mixtures. Individual samples (NVP and excipients) as well as physical mixtures of NVP and selected excipients (all passed through a 60-mesh sieve) were weighed directly in the pierced DSC aluminium pan and scanned in the temperature range of $20\text{--}300^\circ C$ under an atmosphere of dry nitrogen. The heating rate of $10^\circ C/\text{min}$ was used and thermograms obtained were observed for any interaction [7,11].

3.3.4 In-vitro drug release study

The *in-vitro* drug release from nanoparticle formulations was studied across cellulose membranes using Keshary-Chien diffusion cell [12] with an effective diffusional surface area of 1.54 cm^2 and a receptor cell volume of 100 mL. The receptor compartment was filled with the phosphate buffered saline (PBS, pH 4.5) at $37^\circ C$ with constant magnetic stirring. 2 mg of nanoparticle formulations was placed on the donor compartment and covered with a piece of aluminium foil to prevent drying out. The samples (3 mL) were collected from the receptor compartment at the predetermined time interval for 8 h period and replaced by equal volume of fresh prewarmed receptor solution to maintain constant volume allowing sink condition throughout the experiment. The amounts of NVP in the samples were by HPLC.

4.0 HPLC analysis

HPLC analysis of NVP was quantified in samples using high-performance liquid chromatography (HPLC). The

HPLC system consisted of a Dual pump (Model M515, Waters Corp., Milford, MA, USA) and UV-Visible detector (Model M2489, Waters Corp., USA) set at a wavelength of 230 nm. The samples were chromatographed on a reverse-phase NOVA-PAK HR C18 column (4 μm, 150 × 3.9 mm i.d.), (Waters Corp., USA). A mixture of methanol, acetonitrile and buffered solution at pH 3.0 with orthophosphoric acid at 20:20:60 ratios, respectively, was used as the mobile phase. The mobile phase was filtered through a 0.45-μm membrane filter and degassed under vacuum and was pumped at a flow rate of 1 ml/min for the runtime of 10 min, under these experimental conditions 20 μl of the sample solution was injected by Rheodyne Injector (Model 7725i, Waters Corp., USA). The column was thermostated at ambient temperature (40°C) [13].

5.0 Optimization Data Analysis and Validation of the Optimization Model

Various response surface methodology (RSM) computations for the current optimization study were performed employing Design Expert software (Version10.0.4.0, state-Ease Inc, Minneapolis, MN). Polynomial models including interaction and quadratic terms were generated for all the response variables using multiple linear regression analysis (MLRA) approach. The general form of the MLRA model is represented as the following equation.

$$Y = \beta_0 + \beta_1X_1 + \beta_2X_2 + \beta_3X_1X_2 + \beta_4X_1^2 + \beta_5X_2^2 + \beta_6X_1X_2^2 + \beta_7X_1^2X_2$$

Where, β₀ is the intercept representing the arithmetic average of all quantitative outcomes of 9 runs; β₁ to β₇ are the coefficients computed from the observed experimental values of Y, and X₁ and X₂ are the coded levels of the independent variables. The term X₁X₂ and X_i² (i = 1 to 2) represent the interaction and quadratic terms, respectively. The statistical validity of the polynomials was established on the basis ANOVA provision in the Design Expert software. Subsequently, the feasibility and grid search was performed to locate the composition of optimum formulations [14, 15] and the 3-D response surface graphs and counter plots were constructed by Design Expert software. By intensive grid search performed over the whole experimental region, eight optimum checkpoint Formulations were selected to validate the chosen experimental domain and polynomial equations. The

formulations corresponding to these check points were prepared and evaluated for various response properties. The optimized checkpoint formulations were prepared and evaluated for various response properties. Subsequently, the resultant experimental data of response properties were quantitatively compared with that of the predicted values (obtained from Design Expert). Also, linear regression plots between observed and predicted values of response properties were produce using MS-Excel, passing the line through the origin.

5.1 Evaluation of optimized batch formulation

5.1.1 Ex-vivo permeation study

This study was carried out using porcine vaginal mucosa because porcine vaginal mucosa seems good *in vitro* permeability model for human vaginal mucosa [16]. The vaginal tissue was collected from the local slaughter house (Azara, Guwahati, India) and was frozen by placing them in containers with a phosphate buffer saline pH 4.5 (PBS) mixture and stored at -20°C until use. Prior to the experiment, frozen porcine vaginal tissue specimens were thawed in Krebs solution for 1 h at 37°C. Subsequently, the vaginal tissues were dermatomed at a thickness of 300 ± 50 μm and mounted on the Keshary-Chien diffusion cell with an effective diffusional surface area of 1.54 cm² and a receptor cell volume of 100 mL. The receptor compartment was filled with the PBS solution at 37°C with constant magnetic stirring. 2mg of nanoparticle formulations was placed on the donor compartment and covered with a piece of aluminium foil to prevent drying out. The samples (3 mL) were collected from the receptor compartment at the predetermined time interval for 8 h period and replaced by equal volume of fresh prewarmed receptor solution to maintain constant volume allowing sink condition throughout the experiment. The amounts of NVP in the samples were by HPLC. Apparent permeability coefficient (P_{app}) values were calculated from permeability data according to the following equation [17].

$$P_{app} = \frac{Q}{A \times C \times t} \dots\dots\dots (3)$$

Where Q is the total amount of permeated drug (μg), A the diffusion area (cm²), C the initial concentration of drug in the donor compartment (μg/mL) and t the total time of the experiment(s).

Table 1: 3² Factorial Designs of NVP loaded Chitosan Nanoparticle

Formulation Code Trial No		Coded factor level	
		X1	X2
MF1	1	-1	-1
MF2	2	-1	0
MF3	3	-1	1
MF4	4	0	-1
MF5	5	0	0
MF6	6	0	1
MF7	7	1	-1
MF8	8	1	0
MF9	9	1	1
Translation of coded levels in Actual units			
Coded level	-1	0	1
X1:Chitosan (mg)	20	30	40
X2:MgCl ₂ (mg)	60	90	120

Table 2: The composition of NVP loaded Chitosan Nanoparticles

Ingredients (mg)	MF1	MF2	MF3	MF4	MF5	MF6	MF7	MF8	MF9
Nevirapine (NVP)	200	200	200	200	200	200	200	200	200
Chitosan	20	20	20	30	30	30	40	40	40
MgCl ₂	20	60	120	20	60	120	20	60	120
Acetone	35	35	35	35	35	35	35	35	35
PVA	50	50	50	50	50	50	50	50	50

5.1.2 Scanning electron microscopy (SEM)

The surface morphology of the drug-loaded nanoparticles was observed using scanning electron microscopy (SEM) JSM-6360 (JEOL Inc., Japan). The nanoparticle sample was thinly sprinkled onto a metal stub and vacuum coated with a thin layer of gold in an argon atmosphere. The SEM photomicrographs of the coated particles were obtained at 15 kV using a ZEISS, Germany, scanning electron microscope [18].

5.1.3 Physical stability studies of optimized batch formulation

The physical stability of the optimized formulation was carried out on storage at 4°C (refrigerator), 25°C (room temperature) and 40°C (stability chamber) for 6 months. Particle size diameter (PSD), zeta potential, % encapsulation efficiency and % drug release measurements were selected as suitable parameters for the evaluation of physical stability [19,20].

6. RESULTS AND DISCUSSION

6.1 Physico-chemical characterization of NVP loaded nanoparticles

Results of physicochemical characterization of NVP loaded Chitosan nanoparticles were shown in (Table 3). The measured average particle sizes of the formulations were found in the range from 110.1 ± 7.12 to 206.4 ± 8.24 nm with a polydispersity index (PI) in the range of 0.461 ± 0.002 to 0.252 ± 0.004 . The particle size of nanoparticles was varied with a change in drug to polymer ratio in the formulations, with increasing the polymer content average particle size was increased proportionately [21]. The low value of PI revealed uniform size distribution of particles.

The average yields of nanoparticles were about $74 \pm 1.1\%$ to $99 \pm 1.0\%$ and encapsulation efficiency of $61.72 \pm 2.2\%$ to $83.02 \pm 4.8\%$. The average loading and encapsulation efficiency in the formulations were found to increase with an increase in polymer concentration used in the formulations. The results showed NVP-loaded chitosan nanoparticles had zeta potential value of -14.14 to -26.13 mV. The net negative surface charge of all formulations may be due to the use cationic polyelectrolyte (Chitosan) and the addition of polyvinyl alcohol in the formulation aids to reduce aggregation of nanoparticles may indicate the good stability of the formulations [22]. The average droplet of the selected formulation MF6 by dynamic light scattering determination was -14.14 mV.

6.2 Drug-excipient compatibility study

Analysis of drug-excipients compatibility study was carried out by FT-IR and DSC. The FT-IR spectra (Fig. 2) of NVP showed characteristics band at 1643.70 cm^{-1} for (C=O stretching, aromatic/cyclic amide); 1464.56 cm^{-1} (C=C stretching, aromatic), 1410.03 cm^{-1} (skeletal vibration stretching), 1288.24 cm^{-1} (C-N, stretching), 1209.63 cm^{-1} (C-H in-plane bending), 2950 cm^{-1} (N-H peak) [23]. These entire characteristics band for NVP were also retained in 1:1 physical mixture of various NVP-excipients mixture (Fig.3). The results indicated the absence of interaction which was further supported by DSC stud [24].

The DSC curve of NVP showed a first endothermic event between 240 and 250°C (Fig. 4 and 5) with a melting temperature of ($T_{\text{onset}} = 245.58^\circ\text{C}$). This endothermic peak was also retained in all the mixture of drug-excipients with a little shifting of the peaks which may be due to the presence of moisture or impurity of the excipient.

Table 3. Independent Formulation Variables and Their Responses

F.Code	Composition		Particle size(nm)	%Encapsulation efficiency	Zeta potential (mV)	%Drug release(at 8 hours)
	Chitosan(mg)	Mgcl ₂ (mg)				
MF1	30	20	180 ± 1.34	76.16 ± 6.12	-18.15	88.12 ± 2.11
MF2	40	20	206 ± 6.39	83.02 ± 4.8	-16.13	84.13 ± 4.14
MF3	30	70	140 ± 3.78	72.42 ± 4.34	-14.14	90.42 ± 1.46
MF4	20	70	120 ± 2.65	65.15 ± 5.28	-26.13	96.19 ± 4.10
MF5	40	70	150 ± 5.79	74.03 ± 4.16	-19.41	89.16 ± 2.73
MF6	40	120	130 ± 3.15	70.13 ± 2.05	-17.12	94.55 ± 2.03
MF6	20	20	200 ± 1.76	79.15 ± 3.23	-21.23	84.15 ± 4.24
MF7	30	120	125 ± 1.92	66.89 ± 2.19	-20.13	96.19 ± 5.62
MF9	20	120	110 ± 5.34	61.52 ± 2.2	-24.15	98.43 ± 3.76

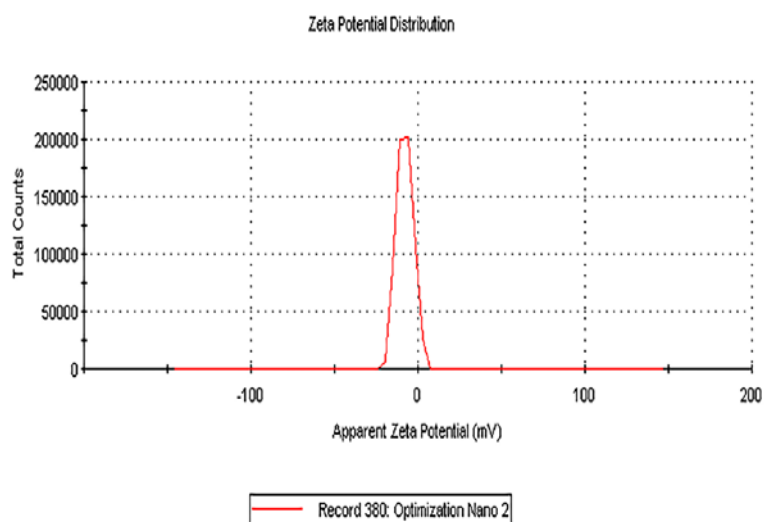


Figure 1: Zeta Potential distribution of optimized formulation.

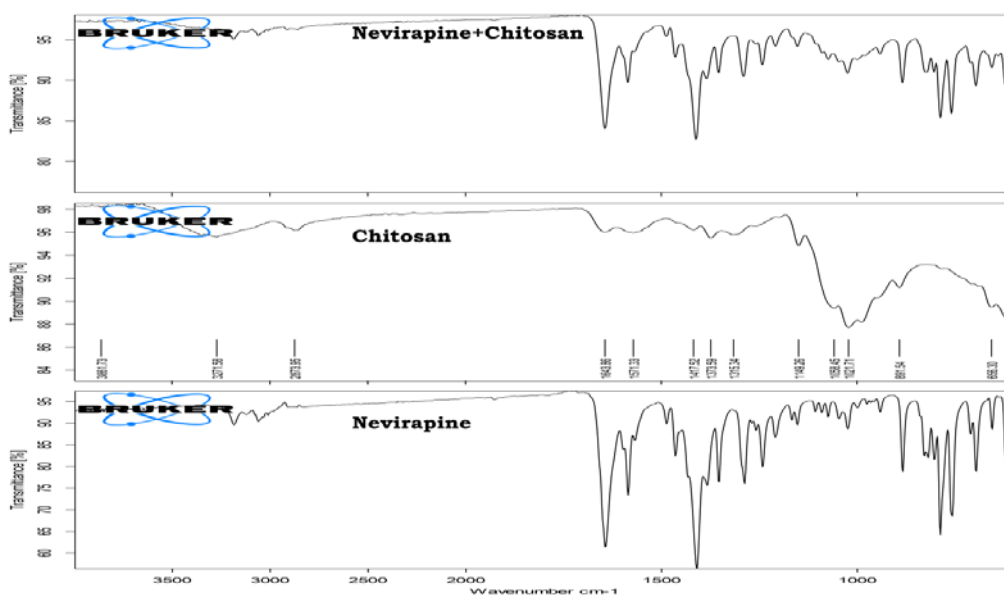


Figure 2: FT-IR Spectra of NVP, Chitosan, Chitosan + NVP.



Figure 3: FT-IR spectra of NVP, polyvinyl alcohol and polyvinyl alcohol+ NVP

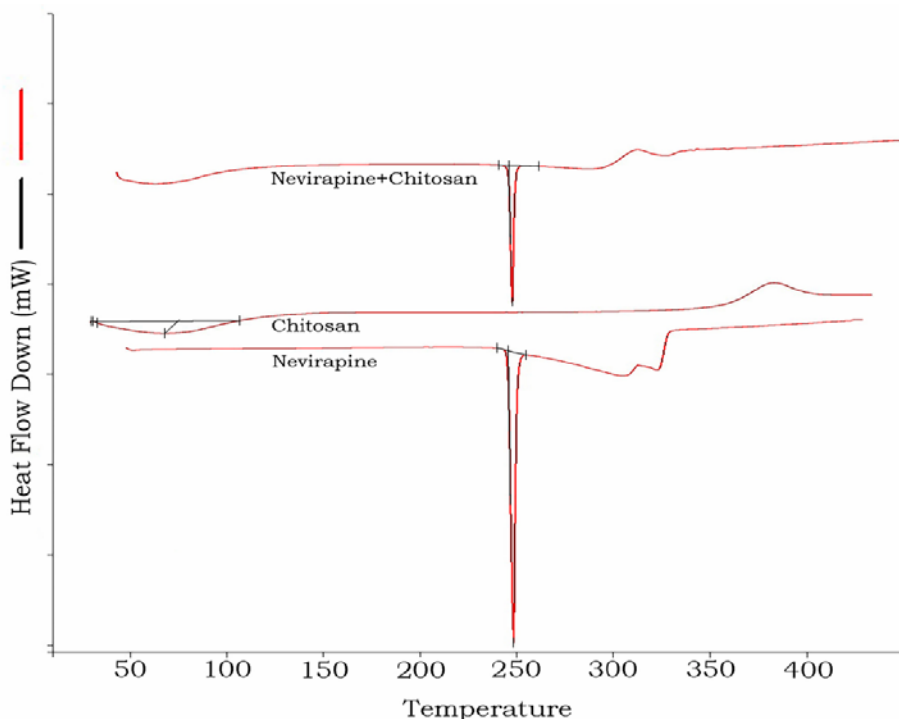


Figure 4: DSC thermogram of NVP, chitosan, NVP + chitosan.

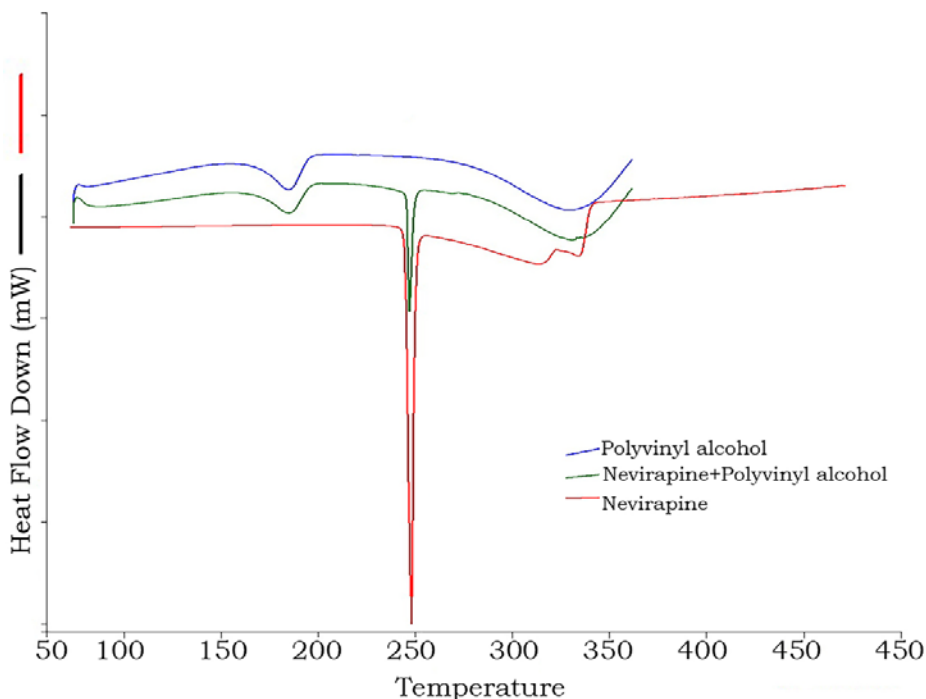


Figure 5: DSC Thermogram of NVP, polyvinyl alcohol, NVP+polyvinyl alcohol

6.3 Statistical Optimization

All the polynomial equations were found to be statistically significant ($P < 0.05$), as determined using ANOVA, as per the provision of Design-Expert software. Quite high values of R^2 of the MLRA coefficients for all four responses, ranging between 0.9411 and 0.9983, vouch for the high prognostic ability of the RSM polynomials

$$Y = \beta_0 + \beta_1X_1 + \beta_2X_2 + \beta_3X_1X_2 + \beta_4X_1^2 + \beta_5X_2^2 + \beta_6X_1X_2^2 + \beta_7X_1^2X_2$$

Seven coefficients (β_1 to β_7) were calculated representing β_0 as the intercept, and β_3 to β_7 various quadratic and

interaction terms. (Table 5) shows the ANOVA results of all response variables indicating model was significant at ($p < 0.05$) for all cases and (Table 4) shows the Polynomial equations of various response variables in terms of coded factors and actual factors. In the actual factors polynomial equations factors which are significant at ($p < 0.05$) are retained in the equations.

Figure 6a to 9a portray the 3-dimensional response surface plots for the studied response properties, viz., particle size(nm), %encapsulation efficiency, zeta potential(mV), % drug release while Figure 6b to 9b depict the

corresponding contour plots. Figure-6a shows the 3-D curve and corresponding counter plot Figure-6b shows a downward trend of wire mesh depicting at a high level (+1) of chitosan concentration. As the concentration of Chitosan increased in the formulation the particle size was significantly increased as the p-values being small at 5% confidence level ($p < 0.05$) and thus revealed that Chitosan had a significant effect on the particle size. Fig.-7a the 3-D curve and corresponding counter plot Fig.-7b shows a downward trend of wire mesh depicting at a high level (+1) for both factors of salting-out agent $MgCl_2$ and Chitosan concentration. As the concentration of either polymer increased in the formulation the % encapsulation efficiency was significantly decreased ($p < 0.05$) and thus it can be evident that polymer Chitosan and $MgCl_2$ had a significant effect on the % encapsulation efficiency of NVP. Figure 8a the 3-D curve and corresponding counter plot Figure 8b shows an upward mesh depicting at a low level(-1) Chitosan concentration and high level(+1) significantly increased zeta potential, thus it indicates that Chitosan and $MgCl_2$ had a significant effect on zeta potential. Figure 9a the 3-D curve and corresponding counter plot Fig. 9b shows a nearly linear descending pattern in *Rel 8 h*, as the content of either polymer is increased, the release of NVP decrease, the effect being much more prominent with Chitosan ($p < 0.05$) than with salting agent ($p > 0.05$).

6.4 Selection of Optimization of the Batch and Validation of RSM Results

The optimum formulation was selected based on the criteria of attaining complete and controlled drug release with minimum particle size. Upon “trading off” various response variables, the following maximum criteria were adopted: particle size < 150 nm, % encapsulation efficiency > 70 %, zeta potential > -15 mV and release of drug at 8 h (*Rel 8 h*) > 90 %.

Upon comprehensive evaluation of feasibility search and subsequently exhaustive grid searches for all nine factorial batches nanoformulation as well as eight checkpoint formulations, the formulation MF6 with the composition of chitosan 40 mg and $MgCl_2$ 120 mg, fulfilled maximum requisites of an optimum formulation. The formulation showed particle size 130 ± 3.15 nm, % encapsulation efficiency 70.13 ± 2.05 %, zeta potential -17.12 and the % drug release at 8 h 94.55 ± 2.03 %. The results of the physical evaluation of the nanoformulation were found to be within the limit. (Table 6) listed the compositions of the checkpoints and optimized formulation [25] their predictive and experimental values of all the response variables and the percentage error are in prognosis. Figure 10 to Figure 13 shows the linear correlation plots between the observed and predictive response variables. Upon comparison of the observed responses with that of the anticipated responses, the prediction error varied between -0.68 % to 7.70 %. The linear correlation plots drawn between the predicted and observed responses demonstrated high values of r^2 (ranging between 0.971 and 0.999), indicating excellent goodness of fit. Upon validation, the optimum formulation exhibited percentage error for various response variables varying between -0.68 and 7.70. Thus the low magnitudes of error, as well as the significant values of r^2 , indicate a high prognostic ability of RSM. The formulation MF6 with the composition of, chitosan 40 mg and $MgCl_2$ 120 mg was selected as optimized formulation and used for the further study.

Table 4: ANOVA Results of Response Variables

Evaluation Parameter	R ² Value	F -Value	P-Value Prob>F	Model Significant/Non Significant Relative to Noise
Particle Size (nm)	0.9562	13.09	0.0299	Significant
Encapsulation efficiency(%)	0.9484	11.04	0.0379	Significant
Zeta potential(mV)	0.9456	10.44	0.0409	Significant
Drug Release (%)	0.9441	10.14	0.0426	Significant

Table 5: Polynomial Equations of Various Response Variables

Evaluation Parameter	Final Equation in Terms of Coded Factor	Final Equation in Terms of Actual Factor
Particle Size(PS)	(PS) = +133.78 + 9.33* A - 36.83* B + 3.50* AB + 4.33* A ² + 21.83* B ²	(PS) = +253.83778 - 2.15667 * Chitosan - 2.16933* $MgCl_2$ + 7.00000E-003* Chitosan * $MgCl_2$ + 0.043333* Chitosan ² + 8.73333E-003* $MgCl_2$ ²
Encapsulation Efficiency(EE%)	(EE%) = +70.75 + 3.23* A - 6.63* B + 1.18* A ⁰ + 0.68* A ² + 1.61* B ²	(EE%) = +84.57909 - 0.24923* Chitosan - 0.29399* $MgCl_2$ + 2.37000E-003* Chitosan * $MgCl_2$ + 6.76667E-003* Chitosan ² + 6.44667E-004* $MgCl_2$ ²
Zeta Potential (mV)(zp)	(ZP) = -20.40 + 2.33* A - 3.50* B + 1.00* AB - 0.25* A ² + 1.27* B ²	(ZP) = -18.05599 + 0.24382* Chitosan - 0.20146* $MgCl_2$ + 2.00500E-003* Chitosan * $MgCl_2$ - 2.51667E-003* Chitosan ² + 5.09333E-004* $MgCl_2$ ²
% Drug Release (% D _{Rel 8h})	(% D _{Rel 8h}) = +93.57 - 2.03* A + 5.85* B - 0.64* AB - 0.80* A ² - 2.49* B ²	(% D _{Rel 8h}) = +76.68644 + 0.36777* Chitosan + 0.29483* $MgCl_2$ - 1.28000E-003* Chitosan * $MgCl_2$ - 8.01667E-003* Chitosan ² - 9.96667E-004* $MgCl_2$ ²

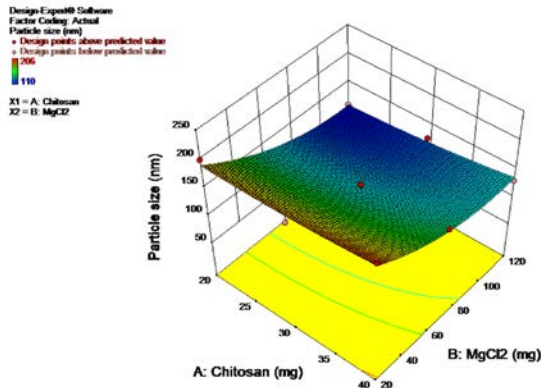


Figure 6a: 3-D response surface plot showing the influence of polymers on Particle Size.

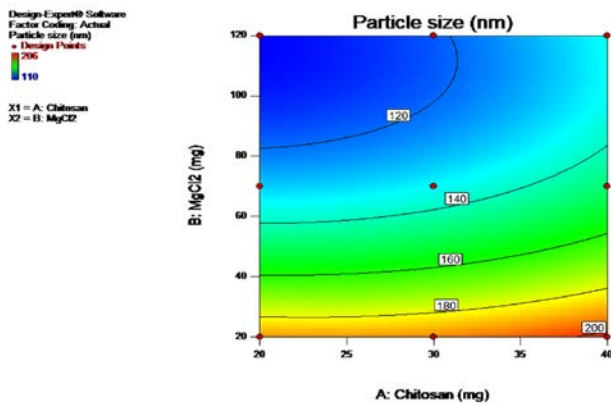


Figure 6b. Counter plot showing the relationship between various levels of two polymers on Particle Size.

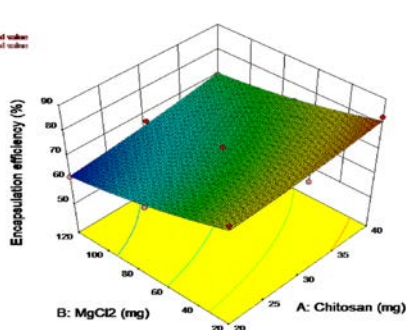


Figure 7a: 3D-Response surface showing the influence of Chitosan and MgCl₂ on Encapsulation efficiency.

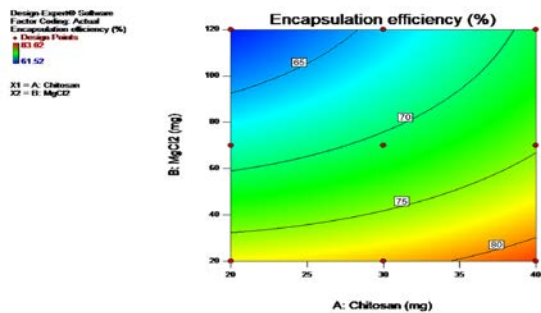


Figure 7b: Counter plot showing the relationship between the various levels of chitosan and MgCl₂ on encapsulation efficiency.

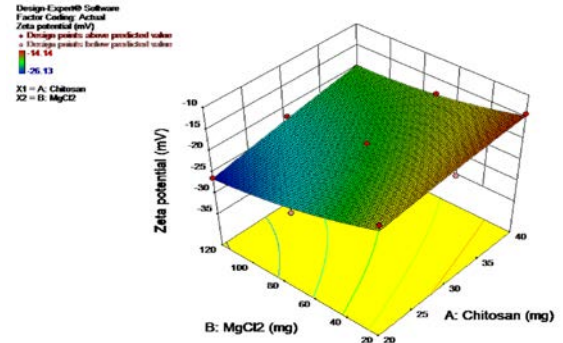


Figure 8a: 3D-Response surface showing the influence of chitosan and MgCl₂ on zeta potential.

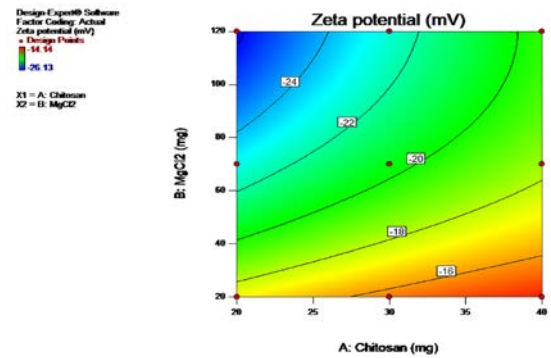


Figure 8b: 3 D-Response surface showing the influence of chitosan and MgCl₂ on zeta potential.

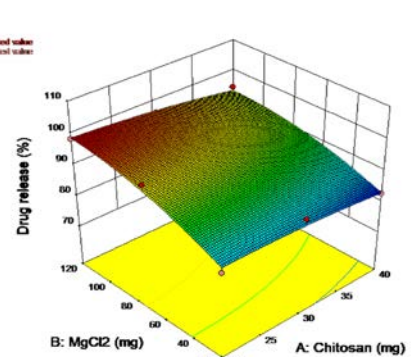


Figure 9a: 3-D response surface plot showing the influence of chitosan and MgCl₂ on % drug release.

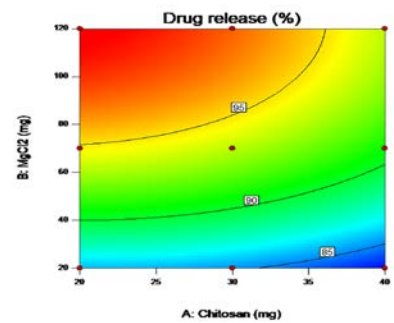


Figure 9b: Counter plot showing the relationship between various levels of chitosan and MgCl₂ on % drug release.

Table 6. The composition of the Optimized and Checkpoint Formulations, the Predicted and Experimental Values of Response Variables and Percentage Prediction Error

Composition (Chitosan:Mgcl ₂)mg	Response Variable	Experimental Value	Predicted Value	Percentage Error
20/20	Particle Size	190.94	190.94	0.71
	%EE	78.54	77.62	1.19
	Zeta potential(mV)	-18.50	-17.21	6.97
	%DR	87.32	85.82	1.71
27.032/44.24	Particle Size	157.82	156.69	0.71
	%EE	74.8	73.87	1.27
	Zeta potential(mV)	-19.83	-18.82	-5.09
	%DR	89.34	90.33	-1.10
20/70	Particle Size	127.31	128.78	-0.68
	%EE	67.31	68.19	1.29
	Zeta potential(mV)	-21.21	-22.98	7.70
	%DR	95.31	94.80	0.53
40/120	Particle Size	134.47	135.94	-1.09
	%EE	69.82	70.81	-1.41
	Zeta potential(mV)	-20.55	-19.55	-4.87
	%DR	92.48	93.45	-1.04
30/120	Particle Size	119.42	118.78	0.53
	%EE	64.31	65.73	-0.022
	Zeta potential(mV)	-23.31	-22.63	-2.16
	%DR	97.54	92.92	0.64
32.21/90.10	Particle Size	123.13	125.09	-1.59
	%EE	70.29	69.19	1.56
	Zeta potential(mV)	-20.01	-21.01	-4.76
	%DR	95.82	94.97	0.886
25.12/46.72	Particle Size	150.90	152.94	-1.35
	%EE	72.53	73.04	-0.703
	Zeta potential(mV)	-20.81	-19.47	-6.43
	%DR	92.49	90.96	2.19
26.09/52.46	Particle Size	147.93	146.85	0.730
	%EE	72.87	72.27	0.82
	Zeta potential(mV)	-18.41	-19.36	4.90
	%DR	93.16	91.80	1.46
28.89/61.22	Particle Size	141.02	141.03	0.72
	%EE	72.63	71.64	1.32
	Zeta potential(mV)	-20.22	-19.99	-1.14
	%DR	94.12	92.68	1.52

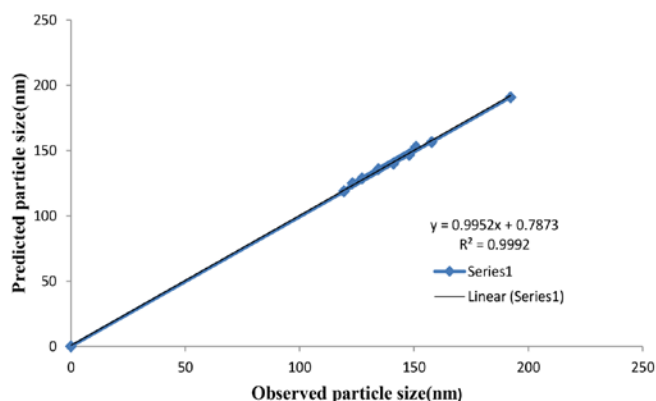


Figure 10: Linear correlation plots between observed and predicted values of particle size (nm).

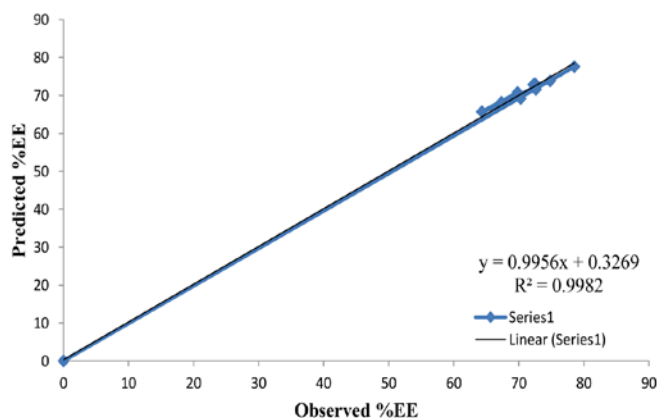


Figure 11: Linear correlation plots between observed and predicted values of encapsulation efficiency (%).

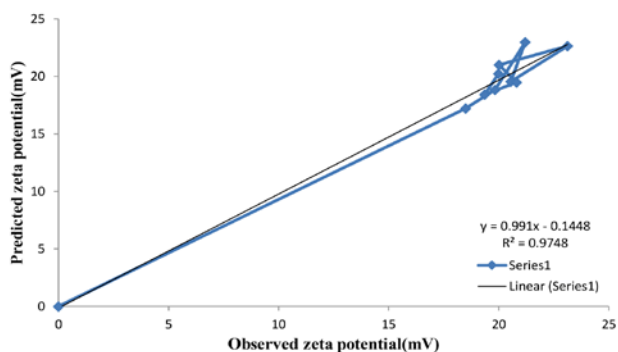


Figure 12: Linear correlation plots between observed and predicted values of Zeta potential (mV).

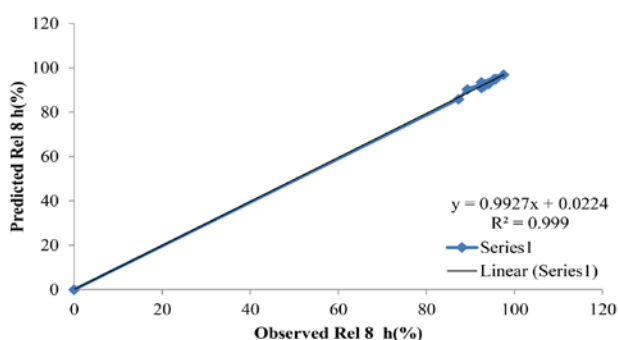


Figure 13: Linear correlation plots between observed and predicted values of Rel 8 h.

6.5 Surface morphology

SEM images of particles (optimized formulation, MF6) as shown in Fig. 14 were spherical in shape with a smooth surface and the size of particles varied from 23.44 nm to 339.5 nm. The particles are discrete and uniform in size and there is no sign of agglomerations confirmed the stability of the formulation. This result is agreement with [26]

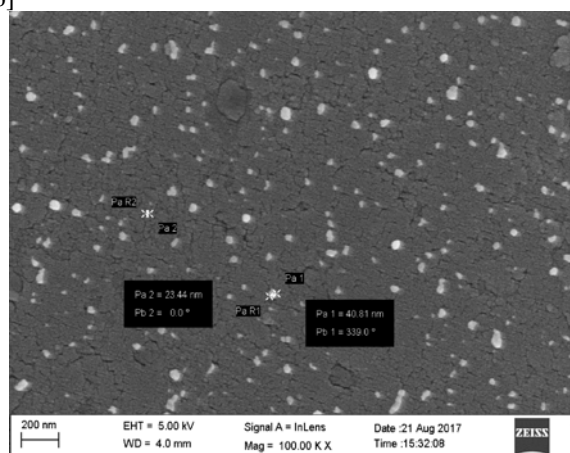


Figure 14.:SEM image of optimized nanoformulation.

Table 7: Permeation parameters of NVP from optimized formulation across porcine mucosa.

F. Code	Amount permeated at 8 h ($\mu\text{g}/\text{cm}^2$) (mean \pm SD)	P_{app} (mean \pm SD)	The best-fit regression equation for permeation plot	r^2
Optimized formulation	1344.40 \pm 43.34	0.084 \pm 32.1 ml $\text{cm}^{-2}\text{h}^{-1}$	Q=0.8811t-0.9839	0.990

6.6. Ex-vivo permeation study

Fig. 15 depicts the *ex-vivo* permeation of NVP through porcine vaginal mucosa. The various permeation parameters were calculated from the permeation profile and presented in (Table 7). The cumulated amount of drug permeated and permeability coefficient was found to be 1344.40 \pm 43.34 μg and 0.084 ml $\text{cm}^{-2}\text{h}^{-1}$ respectively. The best fit regression equation for permeation plot was obtained as Q = 0.8811 t – 0.9839 with r^2 value 0.990. The permeation data was compared with the *in-vitro* release data and the results showed a slight variation in drug permeation rate but which was not observed as statistically significantly ($p > 0.05$). Thus the study confirmed that NVP is easily permeated across the porcine vaginal mucosa which could be meeting the required therapeutics concentration for effective treatment.

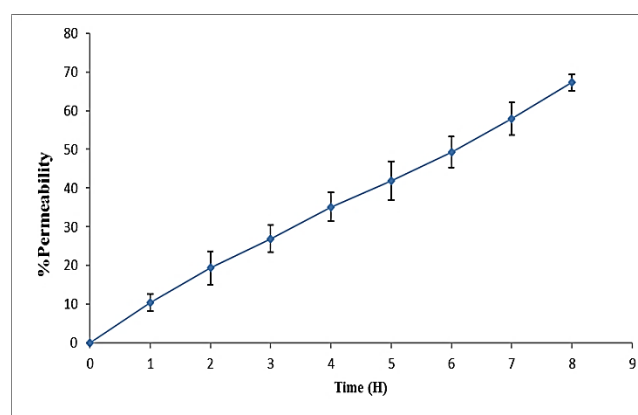


Figure 15. In-vitro permeation study of the optimized batch formulation in phosphate buffer saline solution, pH 4.5 (mean \pm SD, n=2.17)

6.7 Stability study

It has been reported that nanoparticle formulations were prone to aggregation. Hence, the physical stability of the optimized formulation was conducted in various temperature conditions. The results showed in Table 8 revealed that the formulation was physically stable at 4°C (refrigerator), 25°C (room temperature) and 40°C (stability chamber) for 6 months. The measured value of particle size diameter (PSD), zeta potential, % encapsulation efficiency and % drug release at 8 hours were shown in (Table 8). In all the parameters, the measured value was found to remain unchanged (statistically insignificant $p > 0.05$) when compared with the value of the controlled condition (Initial).

Table 8: Results of the stability study for the optimized batch formulation.

Parameter	Controlled condition (Initial)	One month	Three month	Six month
Particle Size (nm)	130±1.4	132.13±3.2	130.19±3.8	131.28±6.5
Zeta potential (mV)	-17.12	-18.01	-18.90	-19.03
% Encapsulation efficiency	74.34±1.2	75.12±3.9	74.49±5.54	75.88±3.9
% Drug Release (at 8 hours)	94.55±4.34	96.13±8.9	95.42±4.7	96.38±4.90

7. CONCLUSION

NVP loaded chitosan nanoparticles were successfully prepared by salting out method using 3² factorial design. The result of FT-IR and DSC study confirmed the absence of incompatibility of NVP with excipients used in the formulations. Data obtained in these studies demonstrated that optimized formulation MF6 showed particle size of 130 ± 3.15 nm with a low polydispersity index of 0.461±0.002, high EE of 83.02 ± 4.8 % and drug release of 94.55 ± 2.03% at 8 hours. Zeta potential value of nanoparticles was found -17.12 mV and SEM images revealed the stability of nanoparticles. The rate of NVP permeation across porcine vaginal mucosa was found to be 168.05 ± 5.41 μ/cm²/hr. In conclusion, stable nanoformulation was developed successfully with very good permeation of the drug across vaginal tissue that may increase the bioavailability in the target area thereby expected to increase the therapeutic effect NVP and will reduce the systemic toxicity. Further, *in-vivo* pharmacokinetics and pharmacodynamic study, safety and efficacy assessment are required to be carried out in future in order to prove the value of proposed nanocarriers.

REFERENCES

- Fauci AS, Folkers GK, Dieffenbach CW. HIV-AIDS: Much accomplished much to do. *Nat Immunol.* 2013;14(11):1104-1107.
- Kallings LO. The first postmodern pandemic: 25 years of HIV/AIDS. *J Intern Med.* 2008; 263(3):218-243
- Antimisiaris SG, Mourtas S. Recent advances on anti-HIV vaginal delivery systems development. *Adv Drug Deliv Rev.* 2015; 1-23.
- Monteiro MSSB, Lunz J, Sebastiao PJ, Tavares MIB. Evaluation of Nevirapine Release Kinetics from Polycaprolactone Hybrids. *Mater Sci Appl.* 2016; 7: 680-701
- Vyas SP, Khar RK. Targeted and controlled drug delivery novel carrier system. CBS Publishers and Distributors Pvt.Ltd. New Delhi. 2002; 345-346.
- Lopez-Leon T, Carvalho ELS, Seijo B, Ortega-Vinuesa JL, Bastos-Gonzalez D. Physicochemical characterization of chitosan nanoparticles: electrokinetic and stability behaviour. *Journal of Colloid and Interface Science.* 2005; 283:344-346.
- Tao Z, Timothy FS, Bi-Botti CY. pH-responsive nanoparticles releasing tenofovir intended for the prevention of HIV transmission. *Eur J Pharm Biopharm.* 2011;79:526-536
- Zhu Z, Li Y, Li X, Li R, Jia Z, Liu B, Guo W, Wu W, Jiang X. Paclitaxel-loaded poly (n-vinylpyrrolidone)- b-poly(ε-caprolactone) nanoparticles: Preparation and antitumor activity in vivo. *J Control Release.* 2010; 142(3):438-446.
- Yangchao L, Boce Z, Wen-Hsing C, Qin W. Preparation, characterization and evaluation of selenite-loaded chitosan/TPP nanoparticles with or without zein coating. *Carbohydrate Polymers.* 2010;82:942-951.
- Ahmed AB, Nath LK. Drug-excipients compatibility studies of nicorandil in controlled release floating tablet. *Int J Pharm Pharm Sci.* 2014;6(2):468-475.
- Adlin JNJ, Anton SA. Preparation and evaluation of stavudine loaded Chitosan Nanoparticles. *J Pharm Res.* 2013;6: 268-274.
- Keshary PR, Chien YW. Mechanism of transdermal controlled nitroglycerin administration. Part 2. Assessment of rate controlling steps. *Drug Develop Ind Pharm.* 1984; 10:1663
- Eunice KK, Cristina HRS, Eunice EMK, Simone SA, Valentina P. Determination of lamivudine in human plasma by HPLC and its use in bioequivalence studies. *Int J Pharm.* 2005;297:73-79.
- Singh B, Ahuja N. Response surface optimization of drug delivery system. *Progress in Controlled and Novel Drug Delivery system.* New Delhi, India: CBS Publishers and Distributors. 2004; 470-509.
- Singh B, Sing SA, a comprehensive computer program for the study of drug release kinetics from compressed matrices. *Indian J Pharm Sci.* 1998; 60: 358-362.
- Eyk VAD, Bijl VP. Porcine vaginal mucosa as an in vitro permeability model for human vaginal mucosa. *Int J Pharm.* 2005;305:105-111.
- Martín-Villena MJ, Fernández-Campos F, Calpena-Campmany AC, Bozal-de Febrer N, Ruiz-Martínez MA, Clares-Naverosa B. Novel microparticulate systems for the vaginal delivery of nystatin: Development and characterization. *Carbohydr Polym.* 2013; 94:1-11.
- Thangaraja A, Savitha V, Jegatheesan K. Preparation and Characterisation of Polyethylene glycol-coated silica nanoparticles for drug delivery application. *IJNA* 2010; 4(1):31-38.
- Sahu BP, Das MK. Nanosuspension for enhancement of oral bioavailability of felodipine. *Appl Nanosci.* 2014; 4:189-197.
- Ankit J, Kanika T, Preeti K, Upendra KJ. Docetaxel-loaded chitosan nanoparticles: Formulation, characterization and cytotoxicity studies. *Int J Biol Macromol.* 2014; 69:546-553.
- Ahmed AB, Konwar R, Sengupta R. Atorvastatin calcium loaded chitosan nanoparticles: in vitro evaluation and in vivo pharmacokinetic studies in rabbits. *Braz J Pharm Sci.* 2015; 51(2):467-478.
- Honary S, Zahir F. Effect of zeta potential on the properties of nano-drug delivery systems—a review (Part 1). *Trop J Pharm Res.* 2013; 12(2):255-64.
- Rampino A, Borgogna M, Blasi P, Bellich B, Cesaro A. Chitosan nanoparticles: Preparation, size evolution and stability. *Int J Pharm.* 2013;455:219-228.
- Jaiswal J, Gupta SK, Kreuter J. Preparation of biodegradable cyclosporine nanoparticles by a high-pressure emulsification-solvent evaporation process. *J Control Release.* 2004; 96:169-178
- Vera Candiotti L, De Zan MM, Cámara MS, Goicoechea HC. Experimental design and multiple response optimization. Using the desirability function in analytical methods development. *Talanta.* 2014; 124:123-38.
- Osuna B, Ponchel G, Vauthier C. Tuning of shell and core characteristics of chitosan-decorated acrylic nanoparticles. *Eur J Pharm Sci.* 2007;30:143-154.